scientific reports

Check for updates

OPEN

Phenomenological model of transthyretin stabilization

Bartek Lisowski[1]✉, Seweryn Ulaszek[1,2], Barbara Wiśniowska[3], Veronika Bernhauerová[4] & Sebastian Polak[1,5]

Transthyretin is a tetrameric transport protein whose monomers, when destabilized, can misfold and form amyloid fibrils, leading to serious diseases like transthyretin amyloidosis cardiomyopathy and neuropathy. While kinetic stabilisers such as tafamidis or acoramidis are designed to prevent tetramer dissociation, clinical data show a puzzling increase in TTR levels after treatment—an effect that our study seeks to investigate by exploring possible underlying mechanisms. Using a simple phenomenological model, we explore whether reduced dissociation alone accounts for this rise or if other mechanisms contribute. We propose that stabilisers may alter TTR clearance by slowing its cellular internalisation or degradation, or even by influencing its synthesis through pharmacological chaperoning. We also examine the role of monomer removal from circulation via re-association into tetramers or through other, possibly pathogenic processes. By integrating pharmacokinetic and pharmacodynamic data with experimental observations, our model provides fresh insights into TTR homeostasis and offers testable predictions for future research. This study highlights the power of simplified, hypothesis-driven models in uncovering biological mechanisms—or, at the very least, in identifying key questions that remain to be answered.

A central assumption in science is that insights from simplified laboratory systems should extend to real-world conditions. Natural observations inspire ideas, tested in controlled settings, and later re-examined in more complex systems. As Anderson noted, "more" is not necessarily better—only different[1]. Forgetting this leads to unnecessary experiments (and the lack of the needed ones), and introduction of artificial parameters instead of using those that can be understood, measured, or deduced. In areas where mechanistic descriptions rapidly branch into layers of poorly constrained assumptions, it is often more productive to adopt a phenomenological perspective: one that captures the empirically observable relationships without committing to unverified mechanistic detail. Such models—frequently overlooked in the life sciences and rarely considered in medicine—are not only simpler than the widely praised mechanistic frameworks, but can be built directly from existing data, offering clarity precisely where excessive mechanistic elaboration obscures rather than illuminates[2,3].

Our focus is transthyretin (TTR), a plasma protein mainly produced in the liver, also secreted by the choroid plexus and pancreas[4–6]. TTR transports thyroxine (T4) and, via retinol-binding protein (RBP), retinol. Functionally, it forms homo-tetramers that reversibly dissociate into monomers[7–10]. In some variants—or even wild-type protein in the elderly—monomers misfold and aggregate into fibrils[11,12] damaging tissues such as heart or nerves[13–15]. Mutant TTR causes hereditary amyloid cardiomyopathy (ATTRv-CM) or neuropathy (ATTRv-PN); wild-type aggregation leads to wild-type cardiomyopathy (ATTRwt-CM)[16].

Amyloid initiation remains unclear—misfolded monomers in blood, internalized tetramers, or intracellular events may be responsible. Nonetheless, stabilizers such as tafamidis and acoramidis slow disease by binding thyroxine sites, preventing dissociation and fibril formation[17,18]. Subunit exchange assays, mixing labelled and unlabelled tetramers in plasma, quantify dissociation and reassociation kinetics, proving key to understanding stabilizer action.

More detailed models have incorporated drug competition with albumin[19,20] and linked binding data, exchange assays, PK, and clinical results. All consistently show a ~ 30% increase in circulating TTR after therapy[17,21,22]. A minimal model we proposed[23] suggested this rise cannot stem solely from slowed dissociation if monomers freely reassociate and are not degraded. By contrast, assuming slow reassociation and rapid

[1]Chair of Pharmaceutical Technology and Biopharmaceutics, Faculty of Pharmacy, Jagiellonian University Medical College, Kraków, Poland. [2]Doctoral School of Medical and Health Sciences, Jagiellonian University Medical College, Kraków, Poland. [3]Department of Social Pharmacy, Faculty of Pharmacy, Jagiellonian University Medical College, Kraków, Poland. [4]Department of Biophysics and Physical Chemistry, Faculty of Pharmacy in Hradec Králové, Charles University, Hradec Králové, Czech Republic. [5]Certara Predictive Technologies (a Certara Company), Level 2-Acero, 1 Concourse Way, Sheffield S1 2BJ, UK. ✉email: bartek.lisowski@uj.edu.pl

monomer clearance readily explains the increase[20]. These opposing outcomes reflect uncertainties in monomer fate, highlighting the need for models that span plausible scenarios and yield testable predictions.

In this study, we examine how kinetic stabilisers[24] raise circulating TTR levels, explicitly considering reversible tetramer dissociation and monomer re-association as shown in subunit exchange experiments. We develop and parameterize PK/PD models of stabiliser action. Despite the biological complexity of TTR interactions with ligands such as retinol-binding protein, thyroxine, and albumin, we show that a phenomenological, data-driven approach can bypass many uncertainties. In particular, subunit exchange assays provide a direct link between stabiliser concentration and the effective reduction in tetramer dissociation, without requiring full knowledge of all binding partners. We focus on wild-type ATTR-CM as the reference case, while noting key differences in variant forms.

To avoid terminological ambiguity, we note that our approach is *phenomenological* only in the sense that certain relationships in the model—most notably the dependence of the tetramer dissociation rate k_d on stabiliser concentration—are inferred directly from experimental subunit-exchange data, without specifying the underlying molecular details like, for example, competitive binding of drug to different proteins. In contrast, the structure of the PK and TTR turnover equations follows standard, physically motivated mass-balance principles and can be viewed as semi-mechanistic. Throughout this work, we therefore use "phenomenological" to denote a data-driven, top-down simplification of mechanistic complexity, not a model devoid of mechanism. This distinction is important: the model retains mechanistic structure where parameters are well-defined, while relying on phenomenological links only where detailed biochemical pathways remain unknown or experimentally inaccessible.

Methods

Transthyretin dynamics

We limit ourselves to the systemic circulation, in which TTR tetramers (T) are assumed to be constitutively produced in the liver and released to circulation at a constant rate r, as shown in Fig. 1. While in blood, TTR tetramers dissociate to and re-associate from monomers (M), with rates k_d and k_a, respectively. It is also removed from blood (via internalization in various tissues, possible degradation and any other potential process leading to a decrease in transthyretin blood level) in a concentration-dependent manner with the rate $k_{rem,T}$. Similarly, monomers are removed at a rate $k_{rem,M}$. Under these assumptions, the dynamics of tetramers and monomers are governed by the following equations:

$$\frac{dT}{dt} = r + k_a M^4 - (k_{rem,T} + k_d)\, T \tag{1}$$

$$\frac{dM}{dt} = 4k_d T - 4k_a M^4 - k_{rem,M}\mathrm{M}. \tag{2}$$

Partial parametrization of this minimal model is possible due to excellent experiments, done in vivo by Jack H. Oppenheimer et al. back in 1960s[25] and more recently in vitro by Frank Schneider et al.[9] and R. Luke Wiseman et al.[26]. The former, namely Oppenheimer et al., in their Table 1, reports measured fractional elimination per day of total TTR tetramers (known previously as thyroxine-binding prealbumin, TBPA) for healthy and hospitalized human subjects, which can be used to estimate $k_{rem,T}$. Knowing serum TTR steady state level and degradation, one can calculate tetramer production (and secretion) rate, r. The value reported in Table 1 was obtained under the assumption that steady-state tetramer concentration is given by $T_{st} = r/k_{rem,T}$ to set a reference point, but this value should be treated with caution (see Sec. 3.1 for details). To convert from TTR mass to concentration,

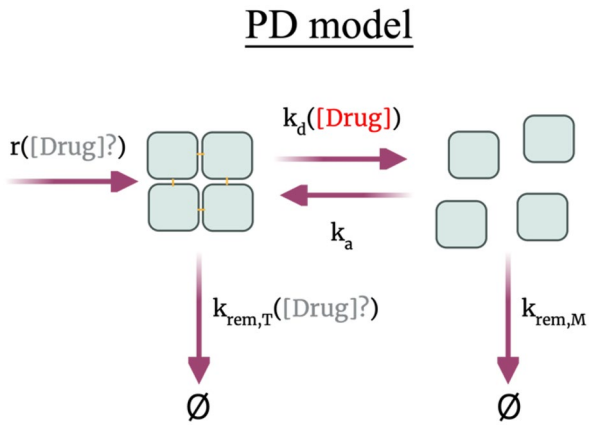

Fig. 1. Scheme of TTR minimal model, showing the transitions for homotetramers and monomers together with corresponding rates (described in the main text). Possible effects, direct and indirect, of action of tetramer stabilisers are denoted as ([Drug]?), while the known stabilisers' effect on tetramer dissociation rate is denoted as $k_d\,([Drug])$.

Parameter	Value	Reference
T_{st}	6.44 μM	subject JO in Table 1 of [25]
r	0.1 $\mu M \times h^{-1}$	calculated as $r = k_{rem,T} T_{st}$ (but see Sec. 3.1)
$k_{rem,T}$	0.016 h^{-1}	subject JO in Table 1 of [25], parameter *K*
k_a	360 000 $\mu M^{-3} \times h^{-1}$	[26], estimated
k_d	0.0024 h^{-1}	data from Fig. 5 in [28] for physiological temperature

Table 1. Values of parameters used in the minimal model of TTR dynamics, which could be measured directly or at least estimated based on experimental data (other parameters—especially $k_{rem,M}$– are discussed in the main text).

transthyretin molecular weight of $M_{TTR} = 55000 \frac{g}{mol}$ was used. We note that it is not always clear whether experimentalists and the kits they use measure only TTR tetramer concentrations or both tetramers and monomers together. Sekijima et al.[27] measured serum monomer concentration, which accounted for much less than 1% of total serum TTR. Therefore, unless otherwise stated, we interpret the experimental values of total TTR as equivalent to tetramer concentrations in the following discussion.

Tetramer dissociation rate has been measured in subunit exchange assays using ATTRwt patients' plasma samples, also in physiological temperature[28]. This technique relies on an assumption, which is supported by observations, that monomer association into tetramers is relatively fast compared to dissociation. Wiseman et al. estimated k_a to be of the order of $10^{20} M^{-3} \times s^{-1} \approx 360000 \mu M^{-3} \times h^{-1}$[26]. All parameter values are shown in Table 1 and discussed in more details in the coming sections.

Pharmacokinetic model

To parametrize PK model, we have used time-drug plasma concentration profile from[29] for the 7th day of therapy with tafamidis single solid oral dosage formulation (61 mg free acid capsules), which was proven bioequivalent to the original tafamidis meglumine formulation (4×20 mg capsules once daily). The data were then fitted using a two-compartmental model, which was sufficient to mimic the pharmacokinetic profile of the drug (see SI):

$$\frac{dm_{GI}}{dt} = -k_{Abs} m_{GI} \tag{3}$$

$$\frac{dc_1}{dt} = \frac{1}{V} k_{Abs} m_{GI} + k_{21} c_2 - (k_{12} + k_{El})\, c_1 \tag{4}$$

$$\frac{dc_2}{dt} = k_{12} c_1 - k_{21} c_2, \tag{5}$$

where m_{GI} is the mass of tafamidis in the gastro-intestinal tract, c_1 and c_2, are tafamidis concentrations in plasma and peripheral compartment, respectively. Transfer rates between compartments and elimination rate are explained in Fig. 2. Volume of the central compartment (i.e., blood plasma), V, needed for converting mass to concentration, is set to be equal to 3000 mL—3/5 of the typical for human 5 L of blood[30]. Since Lockwood et al. report mass concentration, while stoichiometric relationships are defined in terms of molecular counts, in what follows we use molecular weight of tafamidis, $M_{taf} = 308.11 \frac{g}{mol}$, to convert from mass to molar concentrations.

All models were implemented in R Statistical Software (v4.4.2; R Core Team 2024). Nonlinear least-square function, nls(), and FME package were used to fit the parameters[31]. Plots digitization was done with the use of WebPlotDigitizer[32] and figures were partially done in BioRender.

Subunit exchange and drug concentration-tetramer dissociation phenomenological relation.

Phenomenological relation between TTR tetramer stability and tafamidis concentration in physiological temperature was established by Rappley et al.[28]. Using data from their Fig. 5 we have fit the Arrhenius-like relation to capture the dependence of k_d on the plasma concentration of tafamidis, that is c_1 in Eqs. (4) and (5):

$$k_d^{c_1}(c_1) = k_d exp(-\lambda c_1), \tag{6}$$

where $k_d = 0.0024 h^{-1}$ is the rate of dissociation in the absence of drug (i.e., when.

$c_1 = 0$), obtaining for the decay rate $\lambda = 0.112 \frac{1}{\mu M}$, see Fig. 3. Such approach—fitting phenomenological relation given by Èq. (6) (2to data, without detailed knowledge between competing processes, off-target binding etc.—allows to describe tetramer dissociation with minimal set of parameters, among which only λ comes from fitting, while the rest—at least in principle—is well defined and can be obtained experimentally.

Results

Simplicity of pharmacodynamic model contrasts with challenges in parameter estimation

At steady state, Eqs. (1) and (2) reduce to:

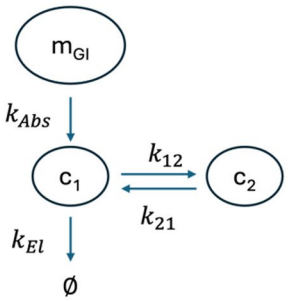

Parameter	Value	Unit
k_{Abs}	0.558	h^{-1}
k_{El}	0.116	h^{-1}
k_{12}	112.070	h^{-1}
k_{21}	22.644	h^{-1}

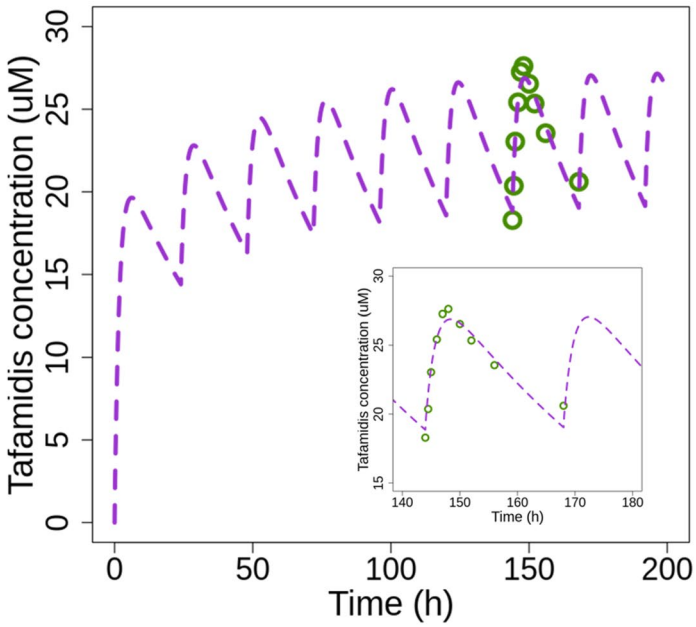

Fig. 2. Tafamidis pharmacokinetics description is based on a two-compartmental model. Data used for parameter fitting are from[29].

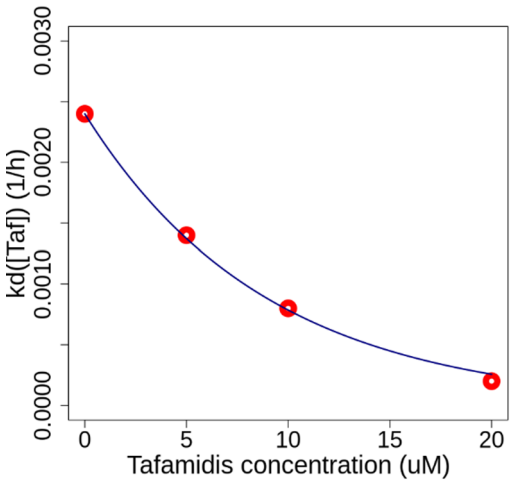

Fig. 3. Phenomenological relation between tetramer dissociation rate and tafamidis concentration. Red dots are experimental results from[28] and blue line is obtained by fitting Eq. (6) (3) to the data, to find best-fit value of $\lambda = 0.112 \frac{1}{\mu M}$.

$$T_{st} = \frac{r + k_a M_{st}^4}{k_{rem,T} + k_d} \tag{7}$$

$$4k_d T_{st} = 4k_a M_{st}^4 + k_{rem,M} M_{st} \tag{8}$$

Here, T_{st} and M_{st} are steady-state tetramer and monomer concentrations, respectively.

Two processes remove monomers from the circulation: reassociation into tetramers ($4k_a M_{st}^4$) and elimination ($k_{rem,M} M_{st}$). At steady state, the balance between these two fluxes controls both the monomer level and, indirectly, the tetramer steady state. A natural consequence of the model is that the flux of reassociation scales with the fourth power of the monomer concentration, whereas monomer degradation is first-order in M. For any oligomerisation pathway, this exponent would reflect the number of monomers that must meet simultaneously (e.g., a dimer would give an M^2 term), and this steep dependence is one of the reasons why the

field generally assumes, although definitive in vivo proof is still lacking, that reassociation is negligible compared to monomer loss under physiological conditions.

When $k_{rem,M} = 0$ (or, more loosely, when the rate of monomer degradation is small compared to reassociation into tetramers and can therefore be neglected), Eq. (8) (5reduces to

$$4k_d T_{st} = 4k_a M_{st}^4, \tag{9}$$

so that

$$\mathrm{M_{st}} = \left(\frac{k_d}{k_a} T_{st}\right)^{\frac{1}{4}}. \tag{10}$$

In this regime, inserting Eq. (10) into Eq. (7) (7(4yields $T_{st} = \frac{r}{k_{rem,T}}$ which is independent of k_d. Reassociation dominates over degradation, and most monomers are recycled back into tetramers.

When degradation dominates over reassociation, most monomers are lost before they can reassemble. Neglecting the reassociation term in Eq (8) (5gives

$$4k_d T_{st} \approx k_{rem,M} M_{st}, \tag{11}$$

Hence

$$\mathrm{M_{st}} \approx \frac{4k_d}{k_{rem,M}} T_{st}. \tag{12}$$

As $k_{rem,M}$ increases, M_{st} becomes smaller, and the contribution $k_a\, M_{st}^4$ in Eq. (7) (4becomes negligible compared to r. The tetramer steady state then approaches

$$T_{st} = \frac{r}{k_{rem,T} + k_d}. \tag{13}$$

In this degradation-dominated regime, lowering k_d directly increases T_{st}.

In the intermediate regime, both processes contribute comparably. For illustration, we consider the case in which the two monomer-removal fluxes are approximately equal,

Because their sum must equal $4k_d T_{st}$ at steady state [cf. Equation (8) (5) and since they are of comparable value, this implies

$$4k_a M_{st}^4 \approx 2k_d T_{st}, \tag{14}$$

or

$$k_a M_{st}^4 \approx 0.5 k_d T_{st}. \tag{15}$$

$$4k_a M_{st}^4 \approx k_{rem,M} M_{st}. \tag{16}$$

Substituting this relation into Eq. (7) (4and rearranging gives

$$T_{st} \approx \frac{r}{\mathrm{k_{rem,T}} + 0.5k_d}, \tag{17}$$

from which the tetramer synthesis rate r can again be recovered.

Having established the steady-state expressions for M_{st} and T_{st} in the reassociation-dominated, degradation-dominated, and intermediate regimes, we can now explore their practical consequences. The key point is that the analytical form of M_{st} and T_{st} depends on the relative magnitudes of the fluxes $4k_a M_{st}^4$ and $k_{rem,M} M$. Knowing several parameters from independent sources—for example, T_{st} and the (assumed, since with a single measurement it cannot be regarded as proven) steady state monomer-to-tetramer ratio $M_{st}/T_{st} \ll 1\%$ from human in vivo measurements, $k_{rem,T}$ from tracer clearance data, k_d with and without stabilisers from subunit exchange experiments, and k_a from kinetic fits—allows us to insert these values into the regime-specific steady-state formulas and solve for the two remaining unknowns, namely the rates of tetramer synthesis, r, and monomer removal, $k_{rem,M}$.

For the reassociation-dominated regime ($4k_a M_{st}^4 \gg k_{rem,M} M_{st}$), the steady state for tetramers reduces to $T_{st} \approx r/k_{rem,T}$, implying $r = k_{rem,T} T_{st}$ and regarding $k_{rem,M}$ negligible. In the degradation-dominated regime ($4k_a M_{st}^4 \ll k_{rem,M} M_{st}$), the tetramer steady state is $T_{st} = r/\left(k_{rem,T} + k_d\right)$, so $r = T_{st}\left(k_{rem,T} + k_d\right)$, and $k_{rem,M}$ follows from the monomer balance. In the intermediate case ($4k_a M_{st}^4 \sim k_{rem,M} M_{st}$), the approximate relation $k_a M_{st}^4 \approx 0.5 k_d T_{st}$ leads to $T_{st} = r/\left(k_{rem,T} + 0.5k_d\right)$, again allowing r to be inferred.

This analysis shows that, while steady-state formulas allow us to back-calculate r, the inferred value depends strongly on which regime is assumed. Direct experimental measurement of either the tetramer synthesis rate r or the monomer removal rate $k_{rem,M}$ would therefore be invaluable: by fixing one of these key parameters, and relying on those we already trust, we could distinguish between the reassociation-, degradation-, and intermediate-dominated regimes and thereby test or falsify some of the underlying assumptions.

Even perfect tetramer stabilisation accounts for only half of the clinical effect

Once the unknown parameters are determined for each regime, we can examine the hypothetical effect of perfect kinetic stabilisation, i.e. eliminating tetramer dissociation ($k_d \to 0$). In the degradation-dominated regime, the relative increase in steady-state tetramer concentration is

$$\frac{T_{st,k_d=0} - T_{st,k_d>0}}{T_{st,k_d>0}} = \frac{k_d}{k_{rem,T}}, \tag{18}$$

which, for the representative parameter set $\left(k_d = 0.0024h^{-1}, k_{rem,T} = 0.016h^{-1}\right)$, corresponds to a maximum possible gain of about 15%. In the intermediate regime, where the effective dependence of T_{st} on k_d is reduced to $(k_{\mathrm{rem,T}} + 0.5\,k_d)$, the maximal gain is halved, while in the reassociation-dominated regime T_{st} is independent of k_d, so no increase is possible. In all three regimes, the relative gain is independent of the inferred tetramer synthesis rate r.

While these estimates already show that dissociation suppression alone cannot account for the > 30% increase in circulating TTR observed clinically, it is important to stress that the inference of several key parameters, most notably the tetramer elimination rate $k_{\mathrm{rem,T}}$ derived from Oppenheimer's tracer data, is itself uncertain and may be biased. If the true $k_{\mathrm{rem,T}}$ were larger or smaller than the value we use, the maximal achievable increase under $k_d \to 0$ would change quantitatively; however, even generous deviations in parameter values cannot raise the theoretical gain anywhere near the clinically observed effect.

These theoretical bounds therefore indicate that additional mechanisms, such as stabiliser-induced changes in TTR clearance, internalisation, degradation, or synthesis, must contribute alongside dissociation suppression to explain the magnitude of the clinical response.

Pharmacokinetic model accurately predicts tafamidis plasma concentration profile

Figure 2 shows tafamidis concentration profile and parameter values predicted by the PK Model described in Sec. 2.2. Two compartmental model, which distinguishes between concentrations in the central c_1 (i.e., blood plasma) and peripheral (i.e., tissues or rest of the body) compartments corresponds well with in vivo data from[29]. Above all, the predicted steady state concentration of tafamidis has a value of around 25 μM, what stays in agreement with drug's specification[33].

Further presentation of the results requires a comment. Here, we limit the use of the PK model to reproducing the total concentration–time profile in plasma, without trying to explain the estimated parameter values. This approach is justified for at least two reasons.

First, TTR is not the only plasma protein capable of binding tafamidis or other stabilisers. For example, while albumin has an order of magnitude lower affinity for tafamidis than TTR, it is at least ten times more abundant. As a result, competition between targets ensures that not all plasma tafamidis is available to bind and stabilize TTR[19].

Second, not all TTR in plasma is fully accessible for stabiliser binding due to its role as a transport protein. Each stabiliser's molecule can bind only to one of the two thyroxine (T4) binding sites on a TTR tetramer. Although most plasma T4 is transported by thyroxine-binding globulin (TBG), up to 15% of TTR molecules have T4 bound to these sites, making them unavailable for stabilisers[34]. Similarly, while the RBP-retinol complex does not sterically block other ligands from binding to the T4 sites, its binding kinetics likely differ from those of an unoccupied TTR tetramer[35–38].

Incorporating these and other molecular details into a physiology-based pharmacokinetic (PBPK) model would surely enhance our understanding of the system. But parametrizing such a model is inherently challenging due to limited available data. This is where a phenomenological approach, paired with the *right* data, provides an effective means to make meaningful progress.

Subunit exchange assay eliminates the impact of known and unknown unknowns

The subunit exchange assay was developed to evaluate the effects of kinetic stabilisers in various types of samples, with its primary advantage being the ability to perform reliable measurements in blood plasma from both healthy individuals and patients with TTR amyloidosis. By tracking the rate at which monomers exchange between labelled and unlabelled tetramers, as well as the distribution of tetramers with different combinations of labelled and unlabelled monomers (e.g., 0 labelled—4 unlabelled, 1 labelled—3 unlabelled, etc.), as a function of a known stabiliser concentration added to donor plasma, it is possible to establish a phenomenological relationship between the tetramer dissociation rate (k_d) and the stabiliser concentration, as shown in Fig. 3.

In a typical subunit exchange assay, recombinant TTR tetramers containing fluorescently or isotopically labelled monomers are mixed with unlabelled TTR present in human plasma. As tetramers transiently dissociate and reassociate, labelled and unlabelled monomers randomly exchange between complexes. The resulting distribution of mixed tetramers (e.g., 1:3, 2:2, 3:1 labelled:unlabelled) is then quantified over time, usually by chromatography or mass spectrometry. Because the rate at which these mixed species appear is directly determined by the underlying tetramer dissociation rate, the assay provides an experimentally accessible readout of kinetic stability under physiologically relevant plasma conditions, even in the presence of endogenous ligands, competing proteins, or stabilisers (whose concentration is controlled by the experimenter).

Crucially, the assay reports the *net* dissociation rate occurring in the full biochemical complexity of human plasma, irrespective of how much stabiliser is free, albumin-bound, or engaged with other proteins. This makes the subunit exchange assay an inherently phenomenological measurement that directly captures the parameter required for PK/PD integration.

Hence, the strength of the resultant relation between tetramer dissociation rate and stabiliser concentration, such as depicted in Fig. 3, lies precisely in this phenomenological character: for a known concentration of a

drug added to blood plasma (with all its known or potential targets) one directly measures the dissociation rate of the TTR tetramer. How much of the drug is bound to tafamidis, T4, or albumin instead of TTR does not matter. This is exactly what is needed to integrate pharmacokinetics (which measures only the total plasma drug concentration, without distinguishing free vs. bound fractions) with pharmacodynamics (which focuses on the effective reduction of tetramer dissociation).

We use tafamidis as an example of a stabiliser due to the availability of data from subunit exchange experiments conducted at physiological temperature[28]. However, this approach is generally applicable to all known and clinically significant stabilisers[19] (see also[39] and[40] for further discussion of the method).

Thus, for an individual patient, performing subunit exchange experiments across several tafamidis concentrations allows fitting of Eq. (3) and direct estimation of the effective decay rate λ. Combined with the patient's pharmacokinetic profile described even by a simple two-compartment model, this enables prediction of tafamidis concentrations over time and, consequently, the extent of TTR stabilization. Because the assay already incorporates the net effects of off-target binding, ligand competition, and variable drug occupancy, these predictions can be made without detailed knowledge of underlying molecular interactions, providing a practical basis for individualized therapy planning.

Discussion and conclusions

In this paper, we stressed the value of drawing maximum insight from existing data, supported by simple quantitative reasoning, while also pointing to key unresolved questions. One central issue is the role of TTR monomers in blood. Their concentration, in vitro and in vivo, represents only a small fraction of total TTR, dominated by tetramers. Yet this observation alone reveals little about the underlying dynamics, much like early misconceptions about HIV replication, which were overturned when Ho, Perelson, Bonhoeffer, Nowak and others showed that viral steady states arise from a balance of production and clearance, leading to the optimization of existing therapies and the development of new ones[41,42].

An analogous approach is needed for TTR. Monomer levels reflect tetramer dissociation opposed by reassociation and elimination, the latter including degradation, amyloid deposition in vessels, or translocation into tissues, collectively described by $k_{rem,M}M$. It is generally assumed that elimination dominates, since reassociation depends on the fourth power of monomer concentration, making it negligible compared to the linear elimination term. This not only determines tetramer steady state but also raises crucial questions about the fate of circulating monomers.

The key uncertainty is that monomer clearance from blood has never been measured directly. By analogy with proteins of similar size, rapid removal seems likely, but this remains unproven. Recent work suggests that dissociation and misfolding of TTR monomers may be constrained by molecular crowding[43]. Protein concentration in healthy human plasma is around 80 g/L. Using the (phenomenological) relation between molar concentration, C, and mean molecular separation in nanometres, $d = 1.18C^{-1/3}$, we estimate that the average distance between plasma proteins is ~ 15 nm[44]. This is only about three to four times the diameter of a TTR monomer (4–5 nm), making it unlikely that dissociated monomers can diffuse far without rapidly encountering other proteins—or each other—suggesting reassociation may be favoured. At the same time, recent reports indicate that amyloid deposits can already form within blood vessels[45]. If the affinity of monomers for such deposits were very high, and the likelihood of encountering them substantial, the "stabilizing" influence of molecular crowding would of course be diminished.

These considerations highlight the importance of analysing the time scales that govern monomer fate after tetramer dissociation. Future studies should measure monomer abundance, tissue penetration, and clearance in health and disease. Notably, other amyloid-forming proteins also exist in oligomeric states[46–49]. Whether such non-linear concentration dependence is a general hallmark of amyloidoses or a coincidence remains an open question.

TTR concentration in blood is one of the few quantitative endpoints used to assess pharmacological stabilisation, though its role as biomarker or prognostic remains debated[50–54]. In ATTRwt and ATTRv patients, TTR concentration has been observed to increase by more than 30% after treatment initiation[17,21,22]. Pharmacodynamic models must account for this effect, yet reduction of tetramer dissociation alone may not suffice in an open system.

In vitro, lowering dissociation stabilises tetramers under mass conservation[23]. In vivo, however, TTR is continually synthesised and cleared by degradation or tissue uptake. Variant TTR removal after liver transplant follows exponential decay, consistent with model predictions[55].

Internalisation adds another layer. Sousa and Saraiva[56] showed that uptake is cell-specific and modulated by ligands: T4 accelerates it, while RBP slows it. Because ligand or drug binding alters TTR conformation, receptors likely sense these changes[57,58]. Although untested, it is plausible that stabilisers such as tafamidis or acoramidis also affect internalisation and possibly other rates as well[59].

Sousa and Saraiva also showed that TTR variants differ markedly in internalisation: the hyper-stable T119M was taken up faster than the amyloidogenic V30M, wild-type TTR, or the highly amyloidogenic L55P, which was barely internalised at all[56]. This highlights how conformational changes strongly affect clearance. Our earlier model assumed stabilisers act only by reducing tetramer dissociation, but it seems equally plausible that binding also alters elimination rate.

Stabilisers target the same tetramer sites as thyroxine, which itself stabilises TTR, and were inspired by the hyper-stable T119M[60,61]. Notably, both T4-bound TTR and T119M are internalised faster than TTRwt[56]. Whether tafamidis or acoramidis have similar effects remains unknown, but such measurements are crucial to understand their impact on TTR turnover. By analogy, stabilisers might even accelerate clearance rather than reduce it.

A further question is whether internalisation always leads to degradation. Sousa and Saraiva observed that hepatic degradation progressed linearly over hours, while internalisation quickly saturated[56]. Thus, uptake and degradation are at least partly decoupled, and reduced $k_{rem,T}$ may result once internalisation plateaus.

Alternatively, could stabilised tetramers be exocytosed back into the circulation, thereby reducing net elimination rate, $k_{rem,T}$? Though untested, evidence suggests cells can favour release of stable tetramers during synthesis and secretion. It is therefore crucial to study tetramer uptake, endothelial transit, degradation, and tissue accumulation, and to determine how stabilisers modulate these processes. Transcytosis could be tested by saturating cells with TTR, then measuring its release into fresh medium. Equally important is understanding TTR production and whether feedback mechanisms exist. Pharmacological chaperoning has been reported[59], but it does not explain how circulating TTR might regulate its own hepatic synthesis—unless internalised TTR acts as an environmental signal, akin to lactose in the lac operon. If so, the assumption of constitutive production would need revision.

Transthyretin amyloidoses pose a major medical and economic burden. Even with improving therapies, late diagnosis and aging populations will sustain the challenge. Advances in models and treatments have clarified ATTR, yet fundamental physiology—TTR secretion, clearance, internalisation, and tissue penetration—remains poorly understood. Closing these gaps is vital for future progress. Moreover, because these processes can be studied in accessible tissues such as blood and even cardiac compartments, unlike the brain, where direct measurement is far more difficult, gaining a deeper understanding of TTR homeostasis may also shed light on general principles relevant to other protein-aggregation disorders. Several neurodegenerative diseases, including Parkinson's and Huntington's disease, involve proteins that form oligomers and aggregates through mechanisms that share conceptual similarities with TTR misfolding. Thus, clarifying the basic physiology of TTR turnover may ultimately benefit not only patients with ATTR, but also help illuminate broader questions in the biology of amyloid diseases.

Data availability

All data generated or analysed during this study are included in this published article and its supplementary information files.

Received: 13 October 2025; Accepted: 1 January 2026
Published online: 09 January 2026

References

1. Anderson, P. W. More is different. *Science* **177**(4047), 393–396. https://doi.org/10.1126/science.177.4047.393 (1972).
2. R. Phillips, 'll Seeing with an extra sense', 2024.
3. Phillips, R. Schrödinger's What Is Life? at 75. *Cell Syst.* **12**(6), 465–476. https://doi.org/10.1016/j.cels.2021.05.013 (2021).
4. C. Sanguinetti *et al.*, 'The Journey of Human Transthyretin: Synthesis, Structure Stability, and Catabolism', 2022, *MDPI*. https://doi.org/10.3390/biomedicines10081906.
5. Refai, E. et al. Transthyretin constitutes a functional component in pancreatic β-cell stimulus-secretion coupling. *Proc. Natl. Acad. Sci.* **102**(47), 17020–17025. https://doi.org/10.1073/pnas.0503219102 (2005).
6. Jacobsson, B., Carlström, A., Platz, A. & Collins, V. P. Transthyretin messenger ribonucleic acid expression in the pancreas and in endocrine tumors of the pancreas and gut*. *J. Clin. Endocrinol. Metab.* **71**(4), 875–880. https://doi.org/10.1210/jcem-71-4-875 (1990).
7. Hamilton, J. A. & Benson, M. D. Transthyretin: A review from a structural perspective. *Cell. Mol. Life Sci.* **58**(10), 1491–1521. https://doi.org/10.1007/PL00000791 (2001).
8. Foss, T. R., Wiseman, R. L. & Kelly, J. W. The pathway by which the tetrameric protein transthyretin dissociates. *Biochemistry* **44**(47), 15525–15533. https://doi.org/10.1021/bi051608t (2005).
9. F. Schneider and J. W. Kelly, 'Transthyretin slowly exchanges subunits under physiological conditions: A convenient chromatographic method to study subunit exchange in oligomeric proteins', 2001, https://doi.org/10.1101/ps.8901.
10. P. Hammarström, 'The Transthyretin Protein and Amyloidosis—an Extraordinary Chemical Biology Platform, 2024, *John Wiley and Sons Inc*. https://doi.org/10.1002/ijch.202300164.
11. Colon, W. & Kelly, J. W. Partial denaturation of transthyretin is sufficient for amyloid fibril formation *in vitro*. *Biochemistry* **31**(36), 8654–8660. https://doi.org/10.1021/bi00151a036 (1992).
12. Quintas, A., Vaz, D. C., Cardoso, I., Saraiva, M. J. M. & Brito, R. M. M. Tetramer dissociation and monomer partial unfolding precedes protofibril formation in amyloidogenic transthyretin variants. *J. Biol. Chem.* **276**(29), 27207–27213. https://doi.org/10.1074/jbc.M101024200 (2001).
13. F. L. Ruberg, M. Grogan, M. Hanna, J. W. Kelly, and M. S. Maurer, 'Transthyretin Amyloid Cardiomyopathy: JACC State-of-the-Art Review', 2019, *Elsevier USA*. https://doi.org/10.1016/j.jacc.2019.04.003.
14. Ruberg, F. L. & Maurer, M. S. Cardiac amyloidosis due to transthyretin protein. *Am. Med. Assoc.* https://doi.org/10.1001/jama.2024.0442 (2024).
15. Grzybowski, J. et al. Diagnosis and treatment of transthyretin amyloidosis cardiomyopathy: A position statement of the polish cardiac society. *Kardiol. Pol.* **81**(11), 1167–1185. https://doi.org/10.33963/v.kp.97648 (2023).
16. D. Adams, H. Koike, M. Slama, and T. Coelho, 'Hereditary transthyretin amyloidosis: a model of medical progress for a fatal disease', 2019, *Nature Publishing Group*. https://doi.org/10.1038/s41582-019-0210-4.
17. Gillmore, J. D. et al. Efficacy and safety of acoramidis in transthyretin amyloid cardiomyopathy. *N. Engl. J. Med.* **390**(2), 132–142. https://doi.org/10.1056/nejmoa2305434 (2024).
18. Bulawa, C. E. et al. Tafamidis, a potent and selective transthyretin kinetic stabilizer that inhibits the amyloid cascade. *Proc. Natl. Acad. Sci.* **109**(24), 9629–9634. https://doi.org/10.1073/pnas.1121005109 (2012).
19. Nelson, L. T. et al. Blinded potency comparison of transthyretin kinetic stabilisers by subunit exchange in human plasma. *Amyloid* **28**(1), 24–29. https://doi.org/10.1080/13506129.2020.1808783 (2021).
20. Tess, D. A. et al. Relationship of binding-site occupancy, transthyretin stabilisation and disease modification in patients with tafamidis-treated transthyretin amyloid cardiomyopathy. *Amyloid* **30**(2), 208–219. https://doi.org/10.1080/13506129.2022.2145876 (2023).
21. S. E. Saith *et al.*, 'Factors associated with changes in serum transthyretin after treatment with tafamidis and outcomes in transthyretin cardiac amyloidosis', 2021, *Taylor and Francis Ltd.* https://doi.org/10.1080/13506129.2021.1904390.

22. Falk, R. H., Haddad, M., Walker, C. R., Dorbala, S. & Cuddy, S. A. M. Effect of tafamidis on serum transthyretin levels in non-trial patients with transthyretin amyloid cardiomyopathy. *JACC CardioOncol.* **3**(4), 580–586. https://doi.org/10.1016/j.jaccao.2021.08.007 (2021).
23. Ulaszek, S., Wiśniowska, B. & Lisowski, B. No body fits in the test tube—The case of transthyretin. *Amyloid* **31**(4), 347–349. https://doi.org/10.1080/13506129.2024.2401154 (2024).
24. E. T. Powers, L. Amass, L. Baylor, I. Fernández-Arias, S. Riley, and J. W. Kelly, 'Transthyretin Kinetic Stabilizers for ATTR Amyloidosis: A Narrative Review of Mechanisms and Therapeutic Benefits', 2025, *Adis*. https://doi.org/10.1007/s40119-025-00423-7.
25. Oppenheimer, J. H., Surks, M. I., Bernstein, G. & Smith, J. C. Metabolism of Iodine-131-labeled thyroxine-binding prealbumin in man. *Science* **149**(3685), 748–751. https://doi.org/10.1126/science.149.3685.748 (1965).
26. Wiseman, R. L., Green, N. S. & Kelly, J. W. Kinetic stabilization of an oligomeric protein under physiological conditions demonstrated by a lack of subunit exchange: Implications for transthyretin amyloidosis. *Biochemistry* **44**(25), 9265–9274. https://doi.org/10.1021/bi050352o (2005).
27. Sekijima, Y. et al. Serum transthyretin monomer in patients with familial amyloid polyneuropathy. *Amyloid* **8**(4), 257–262. https://doi.org/10.3109/13506120108993822 (2001).
28. Rappley, I. et al. Quantification of transthyretin kinetic stability in human plasma using subunit exchange. *Biochemistry* **53**(12), 1993–2006. https://doi.org/10.1021/bi500171j (2014).
29. Lockwood, P. A. et al. The bioequivalence of Tafamidis 61-mg free acid capsules and Tafamidis Meglumine 4 × 20-mg capsules in healthy volunteers. *Clin. Pharmacol. Drug. Dev.* **9**(7), 849–854. https://doi.org/10.1002/cpdd.789 (2020).
30. Yiengst, M. J. & Shock, N. W. Blood and plasma volume in adult males. *J. Appl. Physiol.* **17**(2), 195–198. https://doi.org/10.1152/jappl.1962.17.2.195 (1962).
31. Soetaert, K. & Petzoldt, T. Inverse modelling, sensitivity and Monte Carlo analysis in *R* using package FME. *J. Stat. Softw.* https://doi.org/10.18637/jss.v033.i03 (2010).
32. F. Marin, A. Rohatgi, and S. Charlot, 'WebPlotDigitizer, a polyvalent and free software to extract spectra from old astronomical publications: application to ultraviolet spectropolarimetry', Aug. 2017, [Online]. Available: http://arxiv.org/abs/1708.02025
33. Committee for Medicinal Products for Human Use (CHMP), 'Assessment report - Vyndaquel', Sep. 2011. Accessed: Feb. 12, 2025. [Online]. Available: https://www.ema.europa.eu/en/documents/assessment-report/vyndaqel-epar-public-assessment-report_en.pdf
34. Purkey, H. E., Dorrell, M. I. & Kelly, J. W. 'Evaluating the binding selectivity of transthyretin amyloid fibril inhibitors in blood plasma. *Proc Natl Acad Sci U S A* **98**(10), 5566–5571. https://doi.org/10.1073/pnas.091431798 (2001).
35. Wei, S. et al. Studies on the metabolism of retinol and retinol-binding protein in transthyretin-deficient mice produced by homologous recombination. *J. Biol. Chem.* **270**(2), 866–870. https://doi.org/10.1074/jbc.270.2.866 (1995).
36. Monaco, H., Rizzi, M. & Coda, A. Structure of a complex of two plasma proteins: transthyretin and retinol-binding protein. *Science* **268**(5213), 1039–1041. https://doi.org/10.1126/science.7754382 (1995).
37. Hyung, S.-J., Deroo, S. & Robinson, C. V. Retinol and retinol-binding protein stabilize transthyretin *via* formation of retinol transport complex. *ACS Chem. Biol.* **5**(12), 1137–1146. https://doi.org/10.1021/cb100144v (2010).
38. Raghu, P. & Sivakumar, B. Interactions amongst plasma retinol-binding protein, transthyretin and their ligands: implications in vitamin A homeostasis and transthyretin amyloidosis. *Biochimica et Biophysica Acta BBA Proteins and Proteomics* **1703**(1), 1–9. https://doi.org/10.1016/j.bbapap.2004.09.023 (2004).
39. M. Alhamadsheh, 'Comment to "Nelson LT, Paxman RJ, Xu J, et al. Blinded potency comparison of transthyretin kinetic stabilisers by subunit exchange in human plasma"', 2021, *Taylor and Francis Ltd.* https://doi.org/10.1080/13506129.2020.1853093.
40. J. Kelly and E. Powers, 'Response', 2021, *Taylor and Francis Ltd.* https://doi.org/10.1080/13506129.2020.1853094.
41. Ho, D. D. et al. Rapid turnover of plasma virions and CD4 lymphocytes in HIV-1 infection. *Nature* **373**(6510), 123–126. https://doi.org/10.1038/373123a0 (1995).
42. Wei, X. et al. Viral dynamics in human immunodeficiency virus type 1 infection. *Nature* **373**(6510), 117–122. https://doi.org/10.1038/373117a0 (1995).
43. Jayaweera, S. W. et al. Misfolding of transthyretin *in vivo* is controlled by the redox environment and macromolecular crowding. *J. Biol. Chem.* https://doi.org/10.1016/j.jbc.2024.108031 (2025).
44. Erickson, H. P. 'Size and shape of protein molecules at the nanometer level determined by sedimentation, gel filtration, and electron microscopy. *Biol. Proced. Online.* https://doi.org/10.1007/s12575-009-9008-x (2009).
45. Pedretti, R. et al. Structure-based probe reveals the presence of large transthyretin aggregates in plasma of ATTR amyloidosis patients. *JACC Basic Transl. Sci.* **9**(9), 1088–1100. https://doi.org/10.1016/j.jacbts.2024.05.013 (2024).
46. Bartels, T., Choi, J. G. & Selkoe, D. J. α-Synuclein occurs physiologically as a helically folded tetramer that resists aggregation. *Nature* **477**(7362), 107–111. https://doi.org/10.1038/nature10324 (2011).
47. Sakai, T. et al. Structural and thermodynamic insights into antibody light chain tetramer formation through 3D domain swapping. *Nat. Commun.* https://doi.org/10.1038/s41467-023-43443-4 (2023).
48. Zhu, C., Beck, M. V., Griffith, J. D., Deshmukh, M. & Dokholyan, N. V. Large SOD1 aggregates, unlike trimeric SOD1, do not impact cell viability in a model of amyotrophic lateral sclerosis. *Proc. Natl. Acad. Sci. U S A* **115**(18), 4661–4665. https://doi.org/10.1073/pnas.1800187115 (2018).
49. Torricella, F., Tugarinov, V. & Clore, G. M. Nucleation of huntingtin aggregation proceeds via conformational conversion of pre-formed, sparsely-populated tetramers. *Adv. Sci.* https://doi.org/10.1002/advs.202309217 (2024).
50. Hanson, J. L. S. et al. Use of serum transthyretin as a prognostic indicator and predictor of outcome in cardiac amyloid disease associated with wild-type transthyretin. *Circ. Heart Fail* https://doi.org/10.1161/CIRCHEARTFAILURE.117.004000 (2018).
51. Hood, C. J. et al. Update on disease-specific biomarkers in transthyretin cardiac amyloidosis. *Curr. Heart Fail Rep.* **19**(5), 356–363. https://doi.org/10.1007/s11897-022-00570-1 (2022).
52. Gonzalez-Lopez, E., Maurer, M. S. & Garcia-Pavia, P. Transthyretin amyloid cardiomyopathy: A paradigm for advancing precision medicine. *Eur. Heart J.* https://doi.org/10.1093/eurheartj/ehae811 (2025).
53. Guglielmino, V. et al. Serum biomarkers in transthyretin amyloidosis: An overview of neurofilaments, cardiac, renal, and gastrointestinal involvement. *Neurol. Ther.* **14**(1), 71–84. https://doi.org/10.1007/s40120-024-00696-5 (2025).
54. Adams, D. et al. Expert opinion on monitoring symptomatic hereditary transthyretin-mediated amyloidosis and assessment of disease progression. *Orphanet. J. Rare Dis.* **16**(1), 411. https://doi.org/10.1186/s13023-021-01960-9 (2021).
55. Ando, Y. et al. Change in variant transthyretin levels in patients with familial amyloidotic polyneuropathy type I following liver transplantation. *Biochem. Biophys. Res. Commun.* **211**(2), 354–358. https://doi.org/10.1006/bbrc.1995.1820 (1995).
56. M. M. Sousa and M. J. Saraiva, 'Internalization of transthyretin. Evidence of a novel yet unidentified receptor-associated protein (RAP)-sensitive receptor', In: *Journal of Biological Chemistry*, American Society for Biochemistry and Molecular Biology Inc., Apr. 2001, pp. 14420–14425. https://doi.org/10.1074/jbc.M010869200.
57. Corazza, A. et al. Binding of monovalent and bivalent ligands by transthyretin causes different short- and long-distance conformational changes. *J. Med. Chem.* **62**(17), 8274–8283. https://doi.org/10.1021/acs.jmedchem.9b01037 (2019).
58. B. Basanta *et al.*, 'The conformational landscape of human transthyretin revealed by cryo-EM', 2024. https://doi.org/10.1101/2024.01.23.576879.
59. I. C. Romine and R. L. Wiseman, 'Starting at the beginning: Endoplasmic reticulum proteostasis and systemic amyloid disease', 2020, *Portland Press Ltd*. https://doi.org/10.1042/BCJ20190312.

60. Sekijima, Y. et al. The biological and chemical basis for tissue-selective amyloid disease. *Cell* **121**(1), 73–85. https://doi.org/10.1016/j.cell.2005.01.018 (2005).
61. Miller, M. et al. Enthalpy-driven stabilization of transthyretin by AG10 mimics a naturally occurring genetic variant that protects from transthyretin amyloidosis. *J. Med. Chem.* **61**(17), 7862–7876. https://doi.org/10.1021/acs.jmedchem.8b00817 (2018).

Author contributions

BL, SU and SP conceived the study and designed the model. BL performed the simulations. BL, SU, VB analysed the data. BL, SU, VB, BW contributed to data interpretation and visualization. BL and SU wrote the first draft of the manuscript. All authors reviewed and approved the final version of the manuscript.

Funding

This research was co-funded by the European Union within the VITAL Horizon Europe project (Grant nr 101136728). BL and VB are supported by a grant from the Priority Research Area qLIFE under the Strategic Programme Excellence Initiative at Jagiellonian University under the agreement 06/IDUB/2019/94. VB acknowledges the support of UNCE, project number UNCE/24/MED/008 and the project New Technologies for Translational Research in Pharmaceutical Sciences / NETPHARM, project ID CZ.02.01.01/00/22_008/0004607, co-funded by the European Union.

Declarations

Competing interests

The authors declare no competing interests.

Additional information

Correspondence and requests for materials should be addressed to B.L.

Reprints and permissions information is available at www.nature.com/reprints.

Publisher's note Springer Nature remains neutral with regard to jurisdictional claims in published maps and institutional affiliations.